Limits of the M_1 and M_2 angular moments models for kinetic plasma physics studies

S. Guisset[1,2], J.G. Moreau[2], R. Nuter[2], S. Brull[1], E. d'Humières[2], B. Dubroca[2] and V.T. Tikhonchuk[2]

Abstract. Angular moments closures are widely used in numerical solutions of kinetic equations. While in the strongly collisional limit they are providing a good approximation of the full kinetic equation, their validity domain in the weakly collisional limit is unknown. This work is devoted to define the validity domain of the M_1 model and its extensions, the two populations M_1 and the M_2 angular moments models for the collisionless kinetic physics applications. Three typical kinetic plasmas effects are considered, which are the charged particle beams interaction, the Landau damping and the electromagnetic wave absorption in an overdense semi-infinite plasma. For each case, a perturbative analysis is performed and the dispersion relation is established using the moments models. These relations are compared with those computed by considering the Vlasov equation. The validity limits of each model are demonstrated.

PACS numbers: 52.25.Dg, 52.65.Ff, 52.35.Fp, 52.38.Dx.

1 Introduction

From controlled thermonuclear fusion to space physics, spacecraft propulsion or gas lasers, applications of plasma physics are numerous and diversified. A detailed description of the collisionless plasma dynamics is given by the kinetic Vlasov equation which describes the evolution of the distribution function $f_\alpha(\vec{x}, \vec{v}, t)$ for each particle species α. This function describes the probability of finding particles having the velocity $\vec{v}$ at the position $\vec{x}$ at time t. Such a kinetic description is accurate but also computationally expensive for describing most of real physical applications. An alternative way consists in considering a fluid description based on averaged physical quantities. However, such a macroscopic description is sometimes inaccurate. For example, in the context of inertial confinement fusion, the plasma particles may have an energy distribution far from the thermodynamic equilibrium so that the fluid description is not adapted. Moreover kinetic effects like the non local transport [3, 21], wave damping or the development of instabilities [6] can be important over time scales shorter than the collisional time so that fluid simulations are insufficient and kinetic codes have to be considered to capture the physical processes. Kinetic codes are usually limited to time and length much shorter than those studied with fluid simulations. It is therefore an important challenge to describe kinetic effects using reduced kinetic codes operating on fluid time scales.

The angular moments models represent an alternative method situated between the kinetic and the fluid models. They require computational times shorter than kinetic models ones and provide results with a higher accuraccy than fluid models. They originate from an angular moments average [15, 23] of the kinetic equations. There exist several moment models whose differences come from the choice of the closure relation. The domains of validity of such intermediate models are not strictly defined especially in a weakly collisional limit, and some spurious

[1]Univ. Bordeaux, IMB, UMR 5251, F-33405 Talence, France.
[2]Univ. Bordeaux, CELIA, UMR 5107, F- 33400 Talence, France.

effects may appear. For example, the widespread P_N closure does not ensure the positivity of the distribution function, but can be modified to give a nonnegative closure [11]. In this paper we consider the M_1 and M_2 moments models [7] based on an entropy minimisation principle. The entropy minimisation problems have been widely studied in [15, 23, 24, 26]. The underlying distribution function is given by an exponential of a polynomial function depending on the particle energy and it is therefore nonnegative. Moreover, these closures verify the fundamental mathematical properties [10, 22] such as hyperbolicity and entropy dissipation. However, their solutions could be rather different from the solution of the full kinetic equation. Moreover, from the numerical point of view, even if the closure is well defined, computational challenges remain. In particular, the resolution of the entropy minimization problem can be very computationally costly and we refer to [1] for a specific treatment.

The M_1 model is largely used in various applications such as radiative transfer [28, 2, 9] or electronic transport [18]. It has been shown in [7] that the M_1 model is very accurate in the case of isotropic configurations or with configurations where one direction is dominant. However the model loses precision in the case of an anisotropic configuration and in the limit where the mean free path is larger than the characteristic length of the problem. The accuracy can be improved by considering the two populations M_1 model or the M_2 model [7]. However, their respective domains of validity are not defined either. The aim of this paper is to define the validity domain of the M_1, the two populations M_1 and the M_2 moments models for the kinetic plasma physics applications. The purpose is to investigate if these three moments models are able to capture and describe correctly the basic phenomena occuring in a collisionless plasma. We consider here three classical kinetic effects, which are the interaction of a charged particle beams, the Landau damping of a Langmuir plasma wave and the electromagnetic wave absorption incident normally on a boundary of an overdense plasma. Historically, the two beams instability was one of the first studied plasma physics problems [4, 13]. A beam of charged particles propagates in a plasma generating an oscillating electric field exponentially increasing in time, and reducing the beam kinetic energy. The collisionless damping of plasma waves was first discovered theoretically by Landau [14] then demonstrated in laboratory [5, 20]. The latter physical phenomenon corresponds to the collisionless absorption of an electromagnetic wave incident on an overcritical plasma. A part of the wave energy is absorbed and transfered to the plasma while the other part is reflected [25]. For these three phenomena, a perturbative analysis is performed and the dispersion relation is established using the moments models. These relations are compared in this paper with those obtained directly from the Vlasov equation, providing the accuracy degree of the moments models.

The paper is organised as follows: first we introduce the M_1, the two populations M_1 and the M_2 moments models in Section 2. Then, Section 3 is devoted to the electron beams interaction. A dispersion relation computed with the M_1 model is compared with the one obtained with the Vlasov equation. We highlight that the M_1 model exactly captures the interaction phenomenon. The Landau damping is presented in Section 4. In this case the M_1 model captures the damping qualitatively, but is not able to describe it correctly. On the contrary, the two M_1 populations model and the M_2 model display results with a good accuracy. Then, the collisionless skin effect is studied in Section 5. We show that the M_1 model is not able to describe the absorption phenomenon, while the two populations M_1 model and the M_2 model capture it qualitatively. In order to perform an explicit calculation of the absorption rate, the two limiting cases of a cold and hot electron plasma are studied corresponding to the low and high frequency skin effect [16]. We show that in the cold plasma limit the two populations M_1 and the M_2 moments models give inaccurate absorption coefficients. In the opposite limit the two populations M_1 model fails in describing correctly the phenomenon while the M_2 model provides an accurate result.

2 M_1 and M_2 angular moments models

This section provides a detailed description of the M_1 model [18, 7], the two populations M_1 model [28] and the M_2 model [1, 12]. These three moments models are derived from the kinetic Vlasov equation

$$\partial_t f(t,\vec{x},\vec{v}) + \vec{v}.\nabla_{\vec{x}} f(t,\vec{x},\vec{v}) + \frac{q}{m}(\vec{E}(t,\vec{x}) + \vec{v}\wedge\vec{B}(t,\vec{x})).\nabla_{\vec{v}} f(t,\vec{x},\vec{v}) = 0 \tag{1}$$

where $\vec{E}$ and $\vec{B}$ are the electric and magnetic fields. The constants $q=-e$ and m are the charge and the mass of electron. The electromagnetic fields are computed using the Maxwell's equations

$$\frac{\partial\vec{E}}{\partial t} - c^2\nabla_{\vec{x}}\times\vec{B} = -\frac{\vec{j}}{\varepsilon_0}, \tag{2}$$

$$\nabla_{\vec{x}}.\vec{E} = \frac{q}{\varepsilon_0}(n_e - Zn_i), \tag{3}$$

$$\frac{\partial\vec{B}}{\partial t} + \nabla_{\vec{x}}\times\vec{E} = 0, \tag{4}$$

$$\nabla_{\vec{x}}.\vec{B} = 0 \tag{5}$$

where $n_i = n_0$ is a constant density of single charged ions and the electron density n_e is given by

$$n_e(\vec{x},t) = \int_{\mathbb{R}^3} f(t,\vec{x},\vec{v})d\vec{v}. \tag{6}$$

The electron current $\vec{j}$ is defined by

$$\vec{j}(\vec{x},t) = q\int_{\mathbb{R}^3} f(t,\vec{x},\vec{v})\vec{v}d\vec{v}. \tag{7}$$

2.1 M_1 model

The electronic M_1 model [18, 7] is derived performing an angular moment extraction from the Vlasov equation (1). For the sake of clarity, we omit in the following, the $\vec{x}$ and t dependence of the distribution function. If S^2 is the unit sphere, $\vec{\Omega} = \vec{v}/|\vec{v}|$ represents the direction of propagation of the particle. By setting $\xi = |\vec{v}|$, the distribution function f writes in the spherical coordinates in the phase space $f(\vec{\Omega},\xi)$. Three first angular moments of the distribution function are given by

$$f_0(\xi) = \xi^2\int_{S^2} f(\vec{\Omega},\xi)d\vec{\Omega},\ \ \vec{f_1}(\xi) = \xi^2\int_{S^2} f(\vec{\Omega},\xi)\vec{\Omega}d\vec{\Omega},\ \ \bar{\bar{f}}_2(\xi) = \xi^2\int_{S^2} f(\vec{\Omega},\xi)\vec{\Omega}\otimes\vec{\Omega}d\vec{\Omega}. \tag{8}$$

As performed in [27, 18, 7], the angular integration of the Vlasov equation (1) leads to the following set of equations

$$\begin{cases} \partial_t f_0(\xi) + \nabla_{\vec{x}}.(\xi\vec{f_1}(\xi)) + \frac{q}{m}\partial_\xi(\vec{f_1}(\xi).\vec{E}) = 0, \\ \partial_t\vec{f_1}(\xi) + \nabla_{\vec{x}}.(\xi\bar{\bar{f}}_2(\xi)) + \frac{q}{m}\partial_\xi(\bar{\bar{f}}_2(\xi)\vec{E}) - \frac{q}{m\xi}(f_0(\xi)\vec{E} - \bar{\bar{f}}_2(\xi)\vec{E}) - \frac{q}{m}(\vec{f_1}\wedge\vec{B}) = 0. \end{cases} \tag{9}$$

We assume the unperturbed plasma is isotropic and homogeneous, and the perturbation is in one direction (along the x-axis). In order to describe a perturbation, we select three orthogonal

field components, which correspond to a P-polarized electromagnetic wave. The electromagnetic field has the form

$$\vec{E} = (E_x(x), E_y(x), 0), \vec{B} = (0, 0, B_z(x)). \tag{10}$$

The fundamental point of the moments models is the definition of a closure, which writes the highest moment as a function of the lower ones. This closure relation corresponds to an approximation of the underlying distribution function, which the moments system is constructed from. In the M_1 model (9), we need to define $\bar{\bar{f}}_2$ as a function of f_0 and $\vec{f}_1$. The closure relation originates from an entropy minimization principle [15, 23]. The underlying distribution function f is obtained as a solution of the following minimization problem

$$\min_{f\geq 0}\{\ \mathcal{H}(f)\ /\ \forall \xi \in \mathbb{R}^+,\ \ \xi^2 \int_{S^2} f(\vec{\Omega},\xi) d\vec{\Omega} = f_0(\xi),\ \ \xi^2 \int_{S^2} f(\vec{\Omega},\xi)\vec{\Omega} d\vec{\Omega} = \vec{f}_1(\xi)\ \}, \tag{11}$$

where $\mathcal{H}(f)$ is the Boltzmann entropy defined by

$$\mathcal{H}(f) = \int_{\mathbb{S}^2} (f\ \ln\ f\ -\ f) d\vec{\Omega}. \tag{12}$$

The solution of (11) writes [8, 19]

$$f(\vec{\Omega},\xi) = \exp(\ a_0(\xi) + \vec{a}_1(\xi)\,.\,\vec{\Omega}\ ), \tag{13}$$

where $a_0(\xi)$ is a scalar and $\vec{a}_1(\xi)$ a real valued vector. An important parameter is the anisotropy parameter $\vec{\alpha}$ defined with

$$\vec{\alpha} = \frac{\vec{f}_1}{f_0}. \tag{14}$$

Then the moment $\bar{\bar{f}}_2$ can be calculated [7, 9] as a function of f_0 and $\vec{f}_1$

$$\bar{\bar{f}}_2 = f_0\Big(\frac{1-\chi(\vec{\alpha})}{2}\bar{\bar{I}}_d + \frac{3\chi(\vec{\alpha})-1}{2}\frac{\vec{f}_1}{|\vec{f}_1|}\otimes\frac{\vec{f}_1}{|\vec{f}_1|}\Big) \tag{15}$$

where $\chi(\vec{\alpha})$ is approximated [7] by

$$\chi(\vec{\alpha}) = \frac{1+\vec{\alpha}^2+\vec{\alpha}^4}{3}. \tag{16}$$

The definition (15) enables to close the problem (9).

2.2 Two populations M_1 model

The M_1 model is well adapted to the case of near-isotropic configuration, where $|f_1| << f_0$ ($|\vec{\alpha}| << 1$). In this case it is equivalent to the P_1 model. It provides also a good approximation in the case of one dominant direction ($|\vec{\alpha}| \approx 1$) [7]. However, for the other values of α, the M_1 model may be not sufficiently accurate [7]. In order to improve the accuracy of the model in intermediate cases, it was suggested to decompose the distribution function into two parts. One

part for particles with positive velocities and another one for particles with negative velocities. The total distribution function writes

$$f = f^- + f^+ \tag{17}$$

where $f^- = f|_{v_x<0}$ describes the particle with negative velocities and $f^+ = f|_{v_x>0}$ the particles with positive velocities.

We define the zeroth order angular moments f_0^- and f_0^+.

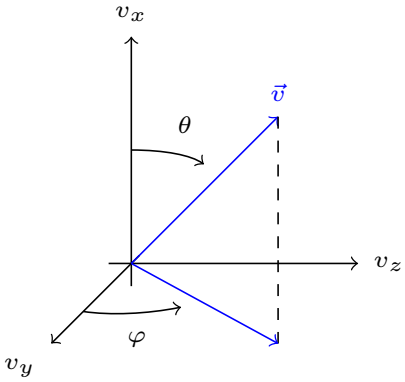

Figure 1: The coordinates system used for the calculation of angular moments of the electron distribution function.

According to (8), the expressions for angular moments write

$$f_0^+(\xi) = \xi^2 \int_0^{2\pi} \int_0^{\pi/2} f(\xi, \vec{\Omega})\ \sin(\theta)\ d\theta d\varphi, \tag{18}$$

and

$$f_0^-(\xi) = \xi^2 \int_0^{2\pi} \int_{\pi/2}^{\pi} f(\xi, \vec{\Omega})\ \sin(\theta)\ d\theta d\varphi. \tag{19}$$

Similarly the first angular moments are defined as

$$\vec{f_1}^+(\xi) = \xi^2 \int_0^{2\pi} \int_0^{\pi/2} f(\xi, \vec{\Omega})\ \vec{\Omega}\ \ \sin(\theta)\ d\theta d\varphi, \tag{20}$$

$$\vec{f_1}^-(\xi) = \xi^2 \int_0^{2\pi} \int_{\pi/2}^{\pi} f(\xi, \vec{\Omega})\ \vec{\Omega}\ \ \sin(\theta)\ d\theta d\varphi, \tag{21}$$

where $\vec{\Omega} = (\cos\theta,\ \sin\theta\cos\phi,\ \sin\theta\sin\phi)$, see Fig.1. Equations (9) are solved for each population distribution. The sum of the two population distributions is considered to compute the electron current $\vec{j}$ (7)

$$\vec{j} = q \int_0^{+\infty} (\vec{f_1}^- + \vec{f_1}^+)\xi d\xi. \tag{22}$$

This source term is considered to solve the Maxwell's equations (2).

2.3 M_2 model

The M_2 model, similarly to the M_1 model is also based on an entropy minimization principle. The difference lies in the fact that an additionnal angular moment is considered making this model more accurate than the M_1 model. Let us introduce the tensor of order three $\vec{\vec{\vec{f}}}_3$

$$\vec{\vec{\vec{f}}}_3(\xi) = \xi^2 \int_{S^2} f(\vec{\Omega}, \xi)\, \vec{\Omega} \otimes \vec{\Omega} \otimes \vec{\Omega}\, d\vec{\Omega}. \tag{23}$$

The entropy minimisation principle for the M_2 model [1, 12] implies that the underlying distribution function writes

$$f(\vec{\Omega}, \xi) = \exp(\ a_0(\xi) + \vec{a}_1(\xi).\vec{\Omega} + \bar{\bar{a}}_2(\xi) : \vec{\Omega} \otimes \vec{\Omega}\ ), \tag{24}$$

where $a_0(\xi)$ is a scalar, $\vec{a}_1(\xi)$ a real valued vector and $\bar{\bar{a}}_2(\xi)$ a real valued tensor of order two. The notation $\otimes$ represents the tensor product and : is the two times contracted product.

The equations of the M_2 model write

$$\begin{cases} \partial_t f_0 + \nabla_{\vec{x}}.(\xi \vec{f_1}) + \frac{q}{m}\partial_\xi(\vec{f_1}.\vec{E}) = 0, \\ \partial_t \vec{f_1} + \nabla_{\vec{x}}.(\xi \bar{\bar{f}}_2) + \frac{q}{m}\partial_\xi(\bar{\bar{f}}_2\vec{E}) - \frac{q}{m\xi}(f_0\vec{E} - \bar{\bar{f}}_2\vec{E}) = 0, \\ \partial_t \bar{\bar{f}}_2 + \nabla_{\vec{x}}.(\xi \vec{\vec{\vec{f}}}_3) + \frac{q}{m}\partial_\xi(\vec{\vec{\vec{f}}}_3\vec{E}) - \frac{q}{m\xi}(\vec{f_1} \otimes \vec{E} + 2\vec{\vec{\vec{f}}}_3\vec{E} + \vec{E} \otimes \vec{f_1}) = 0. \end{cases} \tag{25}$$

The contribution of the self-consistent magnetic field leads to superior order terms in the perturbative analysis and can be neglected because the unperturbed distribution function is isotropic.

3 Particle beam interaction

In this section we study the interaction of electron beams using the M_1 model. We demonstrate that the dispersion relation obtained from the M_1 model agrees exactly with the one obtained from the Vlasov equation.

3.1 Dispersion relation for the M_1 model in the one-dimensional electrostatic case

In the electrostatic case, only one component of the electric field is considered (E_x). The system of equations (9) and the Poisson equation read as

$$\begin{cases} \partial_t f_0 + \partial_x(\xi f_{1x}) - \partial_\xi(E_x f_{1x}) = 0, \\ \partial_t f_{1x} + \partial_x(\xi f_{2xx}) - \partial_\xi(E_x f_{2xx}) + \frac{(f_0 - f_{2xx})E_x}{\xi} = 0, \\ \partial_x E_x = 1 - \int_0^\infty f_0(\xi) d\xi, \end{cases} \tag{26}$$

where the time is normalized to the inverse of the electron plasma frequency $\omega_{pe} = \sqrt{e^2 n_0/m\varepsilon_0}$, the velocity is normalized to the thermal velocity $v_{th} = \sqrt{T/m}$, the length to the Debye length $\lambda_D = v_{th}/\omega_{pe}$, the electric field is normalized to $E_p = m v_{th}\omega_{pe}/e$ and ϵ_0 is the vacuum dielectric permittivity. Only one component of the closure relation (15) is non zero. According to equation (14)

$$f_{2xx} = \chi(\alpha_x) f_0.$$

Let us consider a perturbation of the electric field δE_x and the corresponding perturbation of the zeroth and first moment δf_0 and δf_{1x}

$$\begin{cases} E(t,x) = 0 + \delta E_x(t,x), \\ f_0(t,x,\xi) = F_0(\xi) + \delta f_0(t,x,\xi), \\ f_{1x}(t,x,\xi) = F_{1x}(\xi) + \delta f_{1x}(t,x,\xi), \end{cases} \tag{27}$$

where F_0, F_{1x} correspond to the homogeneous stationary solution of system (26). For the sake of clarity, we omit in the following the arguments t, x and ξ in the equations. The linearized system (26) reads

$$\begin{cases} \partial_t \delta f_0 + \partial_x(\xi \delta f_{1x}) - \partial_\xi(F_{1x}\delta E_x) = 0, \\ \partial_t \delta f_{1x} + \partial_x\left((\chi(\mathcal{F}) - \chi'(\mathcal{F})\mathcal{F})\xi\ \delta f_0 + \chi'(\mathcal{F})\xi\ \delta f_{1x}\right) - \partial_\xi(F_{2xx}\delta E_x) + \frac{(F_0 - F_{2xx})\delta E_x}{\xi} = 0, \\ \partial_x \delta E_x = -\int_0^\infty \delta f_0(\xi) d\xi, \end{cases} \tag{28}$$

where $F_{2xx} = \chi(\mathcal{F})F_0$ and $\mathcal{F} = F_{1x}/F_0$. We define the Fourier transform $\hat{f}$ of a function f as

$$\hat{f}(\omega, k) = \frac{1}{2\pi} \int_{-\infty}^{+\infty} \int_{-\infty}^{+\infty} f(t,x) e^{i(\omega t - kx)} dx dt. \tag{29}$$

The Fourier transform of the first and second equations of (28) results in

$$-i\omega \delta \hat{f}_0 + ik\xi \delta \hat{f}_{1x} = \partial_\xi(F_{1x}\delta \hat{E}_x), \tag{30}$$

$$-i\omega \delta \hat{f}_{1x} + ik\xi(\chi(\mathcal{F}) - \chi'(\mathcal{F})\mathcal{F})\delta \hat{f}_0 + ik\xi\chi'(\mathcal{F})\delta \hat{f}_{1x} = \partial_\xi(\chi(\mathcal{F})F_0 \delta \hat{E}_x) - \frac{(1-\chi(\mathcal{F}))F_0 \delta \hat{E}}{\xi}. \tag{31}$$

For the sake of simplicity, in the following the quantities $\delta \hat{f}$ are replaced by δf. Inserting (30) into (31) gives

$$\delta f_0 = -\frac{1}{iD}\left[(\omega - k\xi\chi'(\mathcal{F}))\partial_\xi F_1 + k\xi\partial_\xi(\chi(\mathcal{F})F_0) - k(1-\chi(\mathcal{F}))F_0\right]\delta E, \tag{32}$$

with

$$D = \omega^2 - \omega k \xi \chi'(\mathcal{F}) - k^2\xi^2[\chi(\mathcal{F}) - \chi'(\mathcal{F})\mathcal{F}].$$

The Fourier transform of the third equation of (26) gives $ik\delta E = -\int_0^\infty \delta f_0(\xi) d\xi$. Then the integration of (32) leads to

$$1 + \int_0^\infty \frac{1}{Dk}\left[(\omega - k\xi\chi'(\mathcal{F}))\partial_\xi F_1 + k\xi\partial_\xi(\chi(\mathcal{F})F_0) - k(1-\chi(\mathcal{F}))F_0\right] d\xi = 0. \tag{33}$$

This equation is the general formulation of the dispersion relation for the M_1 model in the one dimentional electrostatic case. It is applied to the electron beams in the next subsection and to the Landau damping in the next section.

3.2 Electron beams

Let us consider the electron distribution function as a sum of n beams of particles aligned along the x-axis. The distribution function writes

$$f(x,v) = \frac{1}{n}\sum_{l=1}^{n}\delta(v - v_l),$$

where $v_l = \epsilon_l|v_l| = \epsilon_l\xi_l$, with $\epsilon_l = \pm 1$ depending on the direction of propagation of electrons. Now, the corresponding zeroth and first moments F_0, F_1 are given by,

$$F_0(x,\xi) = \xi^2\frac{1}{n}\sum_{l=1}^{n}\delta(\xi - \xi_l),\;\; F_1(x,\xi) = \xi^2\frac{1}{n}\sum_{l=1}^{n}\epsilon_l\delta(\xi - \xi_l).$$

After a simple computation using (16) and the definition of $\mathcal{F}$, we obtain that $\mathcal{F} = \epsilon_l$, $\chi(\mathcal{F}) = 1$ and $\chi'(\mathcal{F}) = 2\epsilon_l$ for $\xi = \xi_l$. Using the previous values in (33), we obtain that $D = (\omega - k\epsilon_l\xi_l)^2 = (\omega - kv_l)^2$, for $\xi = \xi_l$, and the value of the integral in (33) becomes $-\frac{1}{n}\sum_{l=1}^{n} v_l^2/(\omega - kv_l)^2$. We can rewrite the dispersion relation (33) as,

$$1 - \frac{1}{n}\sum_{l=1}^{n}\frac{v_l^2}{(\omega - kv_l)^2} = 0, \tag{34}$$

which agrees exactly with the dispersion relation obtained from the Vlasov equation.

In this part we have shown that the M_1 model correctly describes the particle beams interaction. In the case of different energy beams, the dispersion relation obtained using the M_1 model coincides exactly with the one obtained from the Vlasov equation. It is then evident that more accurate models such as the two populations M_1 model or the M_2 model give the same dispersion equation.
We study in the next part, the Landau damping. It is shown that even if the M_1 model captures qualitatively the phenomenon, it is not accurate enough to describe it quantitatively.

4 Dispersion of an electron plasma wave

Landau damping is a well-known process in plasma physics, which also presents a large interest in some other fields such as galaxy dynamics [17]. The aim of this part is to study if the M_1 model is able to describe the electron plasma wave including the Landau damping effect. We suppose that the equilibrium solution to the Vlasov equation is given by a Maxwellian function

$$f(\xi) = (2\pi)^{-3/2}\exp(-\xi^2/2). \tag{35}$$

The dispersion relation is established from the Vlasov equation in [5]

$$\omega = \sqrt{1 + 3k^2} - \frac{i}{k^3}\sqrt{\frac{\pi}{8}}\exp(-\frac{1}{2k^2}), \tag{36}$$

for small $k << 1$. The negative imaginary part corresponds to the Landau wave damping.

In the following, we perform the dispersion analysis of the Landau wave damping using the three moments models.

4.1 M_1 model applied to the electron plasma wave

In this case, the two first moments are given by,

$$F_0(\xi) = \xi^2 \left(\frac{2}{\pi}\right)^{\frac{1}{2}} \exp(-\frac{\xi^2}{2}), \;\; F_{1x}(\xi) = 0, \tag{37}$$

with $\mathcal{F} = 0$, $\chi(\mathcal{F}) = 1/3$ and $\chi'(\mathcal{F}) = 0$. Using the previous values in (33) we obtain that $D = \omega^2 - k^2\xi^2/3$ and the dispersion relation (33) writes as,

$$1 + \int_0^\infty \frac{\xi \partial_\xi F_0(\xi) - 2F_0(\xi)}{3\omega^2 - k^2\xi^2} d\xi = 1 - \left(\frac{2}{\pi}\right)^{\frac{1}{2}} \int_0^\infty \frac{\xi^4 \exp(-\frac{\xi^2}{2})}{3\omega^2 - k^2\xi^2} d\xi = 0.$$

Using the Landau theory [5] we obtain an approximate dispersion relation assuming a large phase velocity $\omega/k >> 1$ and a weak damping $\mathcal{I}m(\omega) << Re(\omega) \approx 1$. The pole ω/k lies near the real ξ axis, and by using a contour prescribed by Landau with a small semicircle around the pole, the residue formula makes the previous equation equal to

$$1 = -\frac{\sqrt{2}}{\sqrt{\pi}k^2} \left[P \int_0^\infty \frac{\xi^4 \exp(-\frac{\xi^2}{2})}{\left(\xi - \frac{\sqrt{3}\omega}{k}\right)\left(\xi + \frac{\sqrt{3}\omega}{k}\right)} d\xi + i\pi \left. \frac{\xi^4 \exp(-\frac{\xi^2}{2})}{\xi + \frac{\sqrt{3}\omega}{k}} \right|_{\xi = \frac{\sqrt{3}\omega}{k}} \right] \tag{38}$$

where P stands for the Cauchy principal value. As the main contribution to the integral in the case of plasma waves comes from velocities $\xi << \omega/k$, we perform a Taylor expansion for the rational fraction in

$$\frac{1}{\xi^2 - \left(\frac{\sqrt{3}\omega}{k}\right)^2} = -\left(\frac{k}{\sqrt{3}\omega}\right)^2 \frac{1}{1 - \frac{\xi^2}{\left(\frac{\sqrt{3}\omega}{k}\right)^2}} \approx -\left(\frac{k}{\sqrt{3}\omega}\right)^2 \left(1 + \frac{\xi^2}{\left(\frac{\sqrt{3}\omega}{k}\right)^2}\right). \tag{39}$$

Equation (38) then reads

$$1 = \frac{1}{\omega^2} + \frac{5}{3}\frac{k^2}{\omega^4} - \frac{i\sqrt{2\,\pi}}{k^2} \left. \frac{\xi^4 \exp(-\frac{\xi^2}{2})}{\xi + \frac{\sqrt{3}\omega}{k}} \right|_{\xi = \frac{\sqrt{3}\omega}{k}}. \tag{40}$$

We consider the imaginary part of ω as a small perturbation and write

$$\omega = \omega_0 + i\delta\omega \tag{41}$$

with $\delta\omega << \omega_0$. Inserting (41) into (40), neglecting the terms of order $(\delta\omega)^2$ leads to

$$\omega_0^2 + 2i\delta\omega\omega_0 = 1 + \frac{5k^2}{3\omega_0^2}(1 - \frac{2i\delta\omega}{\omega_0}) - if(\omega_0 + i\delta\omega, k). \tag{42}$$

where $f(\omega_0 + i\delta\omega, k) = \dfrac{3\sqrt{6\pi}(\omega_0 + i\delta\omega)^5}{k^5} \exp(\dfrac{-3\omega_0^2}{k^2}) \exp(-\dfrac{6i\delta\omega\omega_0}{k^2})$.

Considering the following linearisation

$$f(\omega_0 + i\delta\omega, k) = f(\omega_0, k) + i\delta\omega f'(\omega_0, k) \tag{43}$$

into (42) and using the fact $\delta\omega << \omega_0$ gives

$$\omega_0^2 = 1 + 5k^2/3 \tag{44}$$

and

$$\delta\omega = -\frac{3\sqrt{6\pi}}{4k^5}\exp(-\frac{5}{2})\exp(-\frac{3}{2k^2}) \approx -\frac{0.267}{k^5}\exp(-\frac{3}{2k^2}). \tag{45}$$

The dissipation found by the M_1 model (45) is signicantly different from the Landau dissipation term (36) computed with the Vlasov equation. Indeed the pre-exponential factor varies in $0.267/k^5$ instead of $0.1398/k^3$ and the coefficient in the exponential is $1/2k^2$ instead of $3/2k^2$. Figure 2 displays the Landau dissipation coefficient as a function of k for the M_1 model (dotted curve) and the Vlasov equation (solid curve). The M_1 model clearly underestimates the Landau dissipation. This figure highlights the impossibility for the M_1 model to accurately model the Landau damping.

4.2 Two populations M_1 model: plasma wave dispersion

We propose here to study the possibility to model the Landau damping with the two populations M_1 model. The stationary solution for the two parts of the distribution function reads

$$f^{\pm}(v) = \frac{1}{(2\pi)^{\frac{3}{2}}}\exp(-\frac{v^2}{2})\mathcal{H}(\pm\cos(\theta)),$$

where $\mathcal{H}$ is the Heaviside function. The corresponding reduced distribution functions are given by,

$$F_0^{\pm}(\xi) = \xi^2\left(\frac{1}{2\pi}\right)^{\frac{1}{2}}\exp(-\frac{\xi^2}{2}), \quad F_{1x}^{\pm}(\xi) = \pm\frac{1}{2}F_0^{\pm}(\xi). \tag{46}$$

The anisotropic coefficients are calculated using (16), $\chi(\mathcal{F}^-) = \chi(\mathcal{F}^+) = 7/16$ and $\chi'(\mathcal{F}^-) = -\chi'(\mathcal{F}^+) = -1/2$. The dispersion relation (33) writes as,

$$\begin{aligned} 0 = 1 \;+\; & \int_0^\infty \frac{1}{\beta^+ k}\left[(\omega - k\xi\chi'(\mathcal{F}^+))\partial_\xi F_1^+ + k\xi\partial_\xi(\chi(\mathcal{F}^+)F_0^+) - k(1-\chi(\mathcal{F}^+))F_0^+\right]d\xi \\ + & \int_0^\infty \frac{1}{\beta^- k}\left[(\omega - k\xi\chi'(\mathcal{F}^-))\partial_\xi F_1^- + k\xi\partial_\xi(\chi(\mathcal{F}^-)F_0^-) - k(1-\chi(\mathcal{F}^-))F_0^-\right]d\xi, \\ = 1 \;+\; & \int_0^\infty \frac{1}{k}\left[\frac{0.661\,\omega^2\xi^2 + 0.079\,\xi^6k^2 + 0.063\,k^2\xi^4 - 0.887\,\xi^4\omega^2}{(\omega^2 - \omega_1^2k^2\xi^2)(\omega^2 - \omega_2^2k^2\xi^2)}\right]F_0^+ d\xi, \end{aligned}$$

where $\beta^{\pm} \approx \omega^2 - 0.199k^2\xi^2 \mp 0.488\ \omega k\xi \approx (\omega \pm \omega_1 k\xi)(\omega \mp \omega_2 k\xi)$ with $\omega_1 = 0.265$ and $\omega_2 = 0.753$.

As the phase velocity $\omega/k >> \xi$, we perform a Taylor expansion of the previous expression to obtain the dispersion relation as for the M_1 model

$$\omega = \sqrt{1 + 2.916k^2} - i\left(\frac{0.19}{k^3} + \frac{0.085}{k^5}\right)\exp(-\frac{0.88}{k^2}),$$

which is close to the dispersion relation (36) obtained from the Vlasov equation. The real part of the dispersion relation is almost exact. Considering the imaginary part, the pre-exponential factor varies in $(0.19/k^3 + 0.085/k^5)$ instead of $0.1398/k^3$ and the coefficient in the exponential is $0.88/2k^2$ instead of $3/2k^2$. The representation of the dissipation coefficient in Fig.2 shows that the two populations M_1 model gives a more accurate result than the previous model for $k < 0.6$. The two populations M_1 model is then a good candidate to model the Landau damping.

4.3 M_2 model

In this part the dispersion relation is established using the M_2 model and compared to the one obtained with the Vlasov equation. It is shown that the M_2 model gives more accurate results than the two populations M_1 model.

In the one dimensional electrostatic case, after normalisation the M_2 model (25) writes

$$\begin{cases} \partial f_0 + \xi \partial_x(f_{1x}) - E_x \partial_\xi(f_{1x}) = 0, \\ \partial_t f_{1x} + \xi \partial_x(f_{2xx}) - E_x \partial_\xi(f_{2xx}) + \frac{E_x}{\xi}(f_0 - f_{2xx}) = 0, \\ \partial_t f_{2xx} + \xi \partial_x(f_{3xxx}) - E_x \partial_\xi(f_{3xxx}) + \frac{E_x}{\xi}(2f_{1x} + 2f_{3xxx}) = 0. \end{cases} \tag{47}$$

The derivation is similar to the one performed for the M_1 model with an additionnal equation. The term f_{2xx} needs to be developed with the perturbative analysis

$$f_{2xx} = F_{2xx} + \delta f_{2xx}. \tag{48}$$

In this case F_{2xx} can be calculated by using the equilibrium state (35)

$$F_{2xx} = F_0/3 \tag{49}$$

with F_0 defined in equation (37). The term f_{3xxx} must be expressed as a function of the other terms. In opposite to the M_1 model closure (15), the M_2 model closure cannot be given explicitly. Nevertheless, using [15, 10, 1] and the equilibrium state (35), the first terms of the development of f_3 are determined. The linearisation of f_{3xxx} results in

$$f_{3xxx} = 0 + \frac{3}{5}\delta f_{1x}. \tag{50}$$

Then the linearisation of (47) gives

$$\begin{cases} \partial_t \delta f_0 + \xi \partial_x(\delta f_{1x}), \\ \partial_t \delta f_{1x} + \xi \partial_x(\delta f_{2xx}) - \frac{1}{3}\partial_\xi(\delta E_x F_0) + \frac{2}{3\xi}\delta E_x F_0 = 0, \\ \partial_t \delta f_{2xx} + \frac{3}{5}\xi \partial_x(\delta f_{1x}) = 0. \end{cases} \tag{51}$$

Following a development similar to the one performed for the M_1 model, the dispersion relation for the M_2 model writes

$$1 = \frac{1}{3}\sqrt{\frac{2}{\pi}} \int_0^{+\infty} \frac{\xi^4}{\omega^2 - k^2\xi^2\lambda} \ \exp(-\frac{\xi^2}{2}) \ d\xi, \tag{52}$$

where the coefficient $\lambda = 3/5$.

Using a contour prescribed by Landau with a small semicircle around the pole, the residue formula applied to the previous equation leads to,

$$1 = \frac{1}{3}\sqrt{\frac{2}{\pi}} \left[P \int_0^{\infty} \frac{\xi^4 \exp(-\frac{\xi^2}{2})}{\omega^2 - k^2\xi^2\lambda} d\xi - \frac{i\pi}{2\omega k\lambda} \ \xi^4 \exp(-\frac{\xi^2}{2}) \Big|_{\frac{\omega}{k\sqrt{\lambda}}} \right]. \tag{53}$$

As the phase velocity $\omega/k >> \xi$, the rational fraction is expanded with a Taylor series

$$\frac{1}{\omega^2 - k^2\xi^2\lambda} = \frac{1}{\omega^2}\Big[1 + \frac{k^2\xi^2\lambda}{\omega^2}\Big]. \tag{54}$$

Then the dispersion relation for the M_2 model reads.

$$\omega = \sqrt{1+3k^2} - i\frac{0.123}{k^5}\exp(-\frac{1.667}{2k^2}). \tag{55}$$

The real part of the dispersion relation is the same as the one obtained with the Vlasov equation. The imaginary part is different, the pre-exponential factor varies in $0.123/k^5$ instead of $0.1398/k^3$ and the coefficient in the exponential is $1.667/2k^2$ instead of $3/2k^2$ but its representation in figure 2 shows a good accuracy of the model.

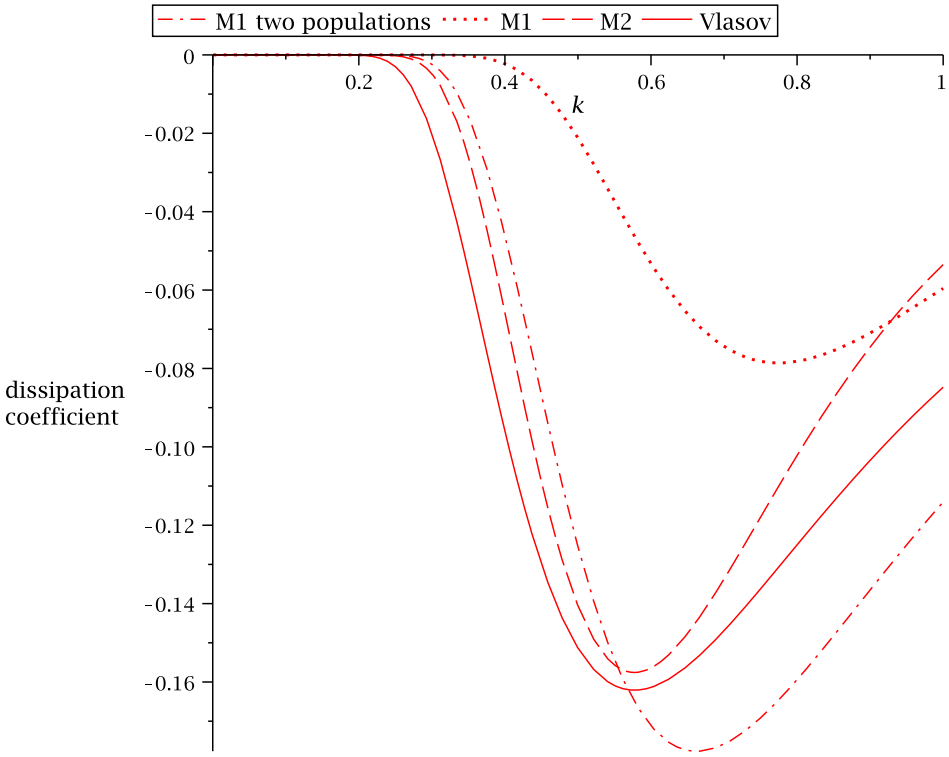

Figure 2: Representation of the dissipation coefficient as a function of k for the Vlasov equation and for the M_1, two populations M_1 and M_2 models.

In conclusion, the dispersion and dissipation of the plasma wave found by using the M_1 model are shown to be inaccurate. One notices in Fig.2 a difference of behavior between the M_1 model and the Vlasov equation. On the contrary, the two populations M_1 model gives much better results with the dissipation term close to the Vlasov dissipation. The M_2 model gives the exact real part of the dispersion relation and it reproduces more accurately than the two populations M_1 model the dissipation.

5 Collisionless skin effect

In contrast to the electrostatic plasma waves, the electromagnetic waves are not damped in a homogeneous collisionless plasma. However, the dissipation appears if the plasma is inhomogeneous. We consider here the case of a plane electromagnetic wave, which is normally incident

on a semi-infinite, overcritical plasma. Here the wave absorption is due to the electrons reflecting from the plasma boundary in a skin layer. The aim of this part is to study how the moments models are able to model such a more complicated situation with an electromagnetic field. The conductivity and absorption coefficient obtained with the M_1, two populations M_1 and M_2 models are compared to the conductivity and absorption coefficient obtained with the Vlasov equation. We consider a low amplitude electromagnetic wave of a frequency ω assuming the linear approach.

Consider a semi-infinite plasma with an electronic density n_0 higher than the critical density $n_c = m\varepsilon_0\omega^2/e^2$. The electromagnetic wave is reflected at the vacuum plasma interface. We propose here to compute the fraction of wave energy absorbed in the plasma [25]. There are two components of the electromagnetic fields E_y and B_z. We suppose the Debye length λ_{De} much smaller than the penetration depth and then the electrons are reflected specularly at $x = 0$. In order to apply the Fourier transform we extend the plasma to the whole space by assuming that an electron coming from $x > 0$, which is reflected in $x = 0$, comes from the fictive region $x < 0$. The study is then extended to the entire space. The electrostatic field E_y is extended as an even function

$$E_y(x) = E_y(-x). \tag{56}$$

The Faraday equation gives

$$\frac{\partial B_z}{\partial t} = -\frac{\partial E_y}{\partial x} \tag{57}$$

the magnetic field is then to be extended as an odd function

$$B_z(x) = -B_z(-x). \tag{58}$$

In this model the electric field is continuous at the surface $x = 0$ but not its first derivative nor the magnetic field. As introduced in [25], the ratio of the electric and magnetic fields at the plasma boundary is characterized by the surface impedance $E(0)/B(0) = \mathcal{Z}$

$$Z = \frac{i\omega}{c\pi}\int_{-\infty}^{+\infty} \frac{dk}{\frac{\omega^2}{c^2} - k^2 + i\omega\mu_0\sigma_{yy}}. \tag{59}$$

where σ is the plasma conductivity. Knowing the impedance one can calculate the absorption coefficient

$$A = \frac{4Re(Z)}{|1+Z|^2} \tag{60}$$

which is related to the real part of the impedance. We suppose that the equilibrium solution is given by the Maxwellian function (35).

5.1 M_1 model for the plasma skin effect

In this part, the conductivity σ and the absorption coefficient A are computed with the M_1 model. We show in this section that the M_1 model is not able to capture the absorption phenomenon.

There is no electromagnetic field and no electron current in the unperturbed plasma. We consider solutions with the perturbation theory. The angular moments are expanded

$$f_0(t,x,\xi) = F_0(\xi) + \delta f_0(t,x,\xi), \tag{61}$$
$$f_{1x}(t,x,\xi) = F_{1x}(\xi) + \delta f_{1x}(t,x,\xi), \tag{62}$$
$$f_{1y}(t,x,\xi) = F_{1y}(\xi) + \delta f_{1y}(t,x,\xi). \tag{63}$$

where F_0 and F_{1x} are given in (37) and $F_{1y} = 0$. The following system corresponds to the M_1 linearised equations

$$\begin{cases} \dfrac{\partial \delta f_0}{\partial t} + \xi \dfrac{\partial \delta f_{1x}}{\partial x} = 0, \\ \dfrac{\partial \delta f_{1x}}{\partial t} + \dfrac{\xi}{3} \dfrac{\partial \delta f_0}{\partial x} = 0, \\ \dfrac{\partial \delta f_{1y}}{\partial t} + \dfrac{q\delta E_y}{3m} \dfrac{\partial F_0}{\partial \xi} - \dfrac{2q\delta E_y F_0}{3m\xi} = 0. \end{cases} \tag{64}$$

The Fourier transform of the last equation of (64) results in an explicit solution for f_{1y}

$$\delta f_{1y} = \frac{iq}{m\omega}\Big[\frac{2F_0}{3\xi} - \frac{1}{3}\frac{\partial F_0}{\partial \xi}\Big]\delta E_y. \tag{65}$$

Considering (22) and (65), the electric current is calculated

$$j_y = \frac{iq^2}{m\omega}\int_{\mathbb{R}^+}\Big[\frac{2F_0}{3} - \frac{\xi}{3}\frac{\partial F_0}{\partial \xi}\Big]d\xi\ \delta E_y. \tag{66}$$

Introducing the conductivity tensor σ such that $j_y = \sigma_{yy}\delta E_y$, the integration by part in equation (66) provides

$$\sigma_{yy} = \frac{ie^2 n_0}{m\omega}. \tag{67}$$

Inserting this expression into equation (59) one obtains the impedance without any real part. Correspondingly there is no absorption,

$$A = 0. \tag{68}$$

Therefore, the M_1 model is not able to correctly model the absorption phenomenon. After linearisation of the M_1 model, we note there is no contribution of the space derivative in the third equation of (64). Then the conductivity (67) does not depend on the wave number k and there is no absorption. This is an important result showing a limitation in the M_1 model for collisionless plasma physics applications. More accurate models need to be used for studies of the electromagnetic wave absorption. The aim of the next section is to make a calculation using the two populations M_1 model.

5.2 Two populations M_1 model

Here, the conductivity and the absorption coefficient are calculated using the two populations M_1 model. We show that this model is able to model the absorption phenomenon but does not capture it quantitatively. In this case the first order moments in the perturbative development

are given by (46) and $F_{1y}^{+} = F_{1y}^{-} = 0$.

The linearisation of the two populations M_1 model leads to

$$\frac{\partial \delta f_{1y}^{\pm}}{\partial t} \mp \xi(3\chi - 1)\frac{\partial \delta f_{1y}^{\pm}}{\partial x} + \frac{q(1-\chi)\delta E_y}{2m}\frac{\partial F_0^{\pm}}{\partial \xi} - \frac{q(1+\chi)F_0^{\pm}\delta E_y}{2m\xi} \pm \frac{qF_0^{\pm}B_z}{2m} = 0 \tag{69}$$

with $\chi = 7/16$. The Fourier transform of equation (69) results in

$$\delta f_{1y}^{\pm} = \frac{q}{2m}\frac{i\Big[\frac{(1+\chi)F_0^{\pm}}{\xi} - (1-\chi)\frac{\partial F_0^{\pm}}{\partial \xi} \mp \frac{F_0^{\pm}k}{\omega}\Big]\delta E_y}{\omega \pm \xi(3\chi - 1)k}. \tag{70}$$

Using the definition of the electric current (22) and the definition of the conductivity in the previous section one obtains

$$\sigma_{yy} = i\frac{q^2}{2m}\int_{\mathbb{R}^+}\Big[\frac{\frac{(1+\chi)F_0}{\xi} - (1-\chi)\frac{\partial F_0}{\partial \xi} - \frac{F_0 k}{\omega}}{\omega + \xi(3\chi-1)k} + \frac{\frac{(1+\chi)F_0}{\xi} - (1-\chi)\frac{\partial F_0}{\partial \xi} + \frac{F_0 k}{\omega}}{\omega - \xi(3\chi-1)k}\Big]\xi d\xi. \tag{71}$$

The calculation of the previous equation leads to

$$\sigma_{yy} = \frac{i\omega_{pe}^2\varepsilon_0}{\sqrt{2\pi}v_{th}^3}\int_{\mathbb{R}}\frac{-\frac{1}{2} + \frac{3}{2}\chi + \frac{k\xi}{2\omega} + \frac{\xi^2(1-\chi)}{2v_{th}^2}}{\omega - \xi(3\chi-1)k}\xi^2\exp(-\frac{\xi^2}{2v_{th}^2})d\xi. \tag{72}$$

The conductivity (72) can not be evaluated analytically. We consider the two limiting cases $\omega/k << v_{th}$ and $\omega/k >> v_{th}$.

5.2.1 Hot electron case

Following the method introduced in the previous section for the calculation of the integral in expression (72) in the limit $\omega/k << v_{th}$ one obtains the following expression for the plasma conductivity

$$\sigma_{yy} = \frac{i\omega_{pe}^2\varepsilon_0}{\sqrt{2\pi}v_{th}^3k^3}\Big[-\frac{4v_{th}^2k^2}{(3\chi-1)^4} - \frac{i\pi\omega^2[(3\chi-1)^2+1]}{2(3\chi-1)^4}\Big]. \tag{73}$$

It has to be compared to the one obtained with the Vlasov equation σ_{yy}^{Vlasov}

$$\sigma_{yy}^{Vlasov} = \frac{i\omega_{pe}^2\varepsilon_0}{\sqrt{2\pi}v_{th}k}\Big[\frac{\omega\sqrt{2\pi}}{kv_{th}} - i\pi\Big]. \tag{74}$$

In contrast to the M_1 model case, the conductivity in this case depends on the wave number k. This difference with the M_1 model originates from equation (69) where there is a contribution of the space derivative, which corresponds to the spatial dispersion. Nevertheless the conductivity obtained with the two populations M_1 model is different from the one obtained with the Vlasov equation. Indeed, ignoring the constant values, the real part of the conductivity varies in $\omega_{pe}^2/v_{th}k$ instead of $\omega_{pe}^2\omega/v_{th}^2k^2$ for the Vlasov equation and the imaginary part varies in $\omega_{pe}^2\omega^2/v_{th}^3k^3$ instead of $\omega_{pe}^2/v_{th}k$ for the Vlasov equation.

Using the fact that $\omega << kv_{th}$ the calculation of the impedance Z leads to

$$Z = -\frac{2i\omega}{c\pi}\int_0^{+\infty}\frac{dk}{k^2 - i\frac{\tilde{K}}{k^3}} \tag{75}$$

with

$$\tilde{K} = \frac{\pi\omega^3\omega_{pe}^2[(3\chi-1)^2+1]}{2\sqrt{2\pi}v_{th}^3c^2(3\chi-1)^4}. \tag{76}$$

The impedance computation results in

$$Z = \frac{2\omega e^{-i\frac{2\pi}{5}}}{5\sin(\frac{\pi}{5})c\sqrt[5]{\tilde{K}}}. \tag{77}$$

Inserting equation (77) into the definition of the absorption coefficient equation (60) leads to

$$A = \frac{K_1\Big(\frac{\omega}{\omega_{pe}}\Big)^{\frac{2}{5}}\Big(\frac{v_{th}}{c}\Big)^{\frac{3}{5}}}{\Big[1+\frac{K_1}{4}\Big(\frac{\omega}{\omega_{pe}}\Big)^{\frac{2}{5}}\Big(\frac{v_{th}}{c}\Big)^{\frac{3}{5}}\Big]^2+\Big[\frac{K_1}{4}\Big(\frac{\omega}{\omega_{pe}}\Big)^{\frac{2}{5}}\Big(\frac{v_{th}}{c}\Big)^{\frac{3}{5}}\Big]^2} \tag{78}$$

with

$$K_1 = \frac{8\cos(\frac{2\pi}{5})}{5\sin(\frac{\pi}{5})}\Big(\frac{2\sqrt{2\pi}(3\chi-1)^4}{\pi(3\chi-1)^2+1}\Big)^{\frac{1}{5}} \approx 0.434. \tag{79}$$

This absorption coefficient has to be compared to the one obtained with the Vlasov equation

$$A^{Vlasov} = \frac{K_2\Big(\frac{\omega}{\omega_{pe}}\Big)^{\frac{2}{3}}\Big(\frac{v_{th}}{c}\Big)^{\frac{1}{3}}}{\Big[1+\frac{K_2}{4}\Big(\frac{\omega}{\omega_{pe}}\Big)^{\frac{2}{3}}\Big(\frac{v_{th}}{c}\Big)^{\frac{1}{3}}\Big]^2+\Big[\frac{K_2}{4}\Big(\frac{\omega}{\omega_{pe}}\Big)^{\frac{2}{3}}\Big(\frac{v_{th}}{c}\Big)^{\frac{1}{3}}\Big]^2} \tag{80}$$

with

$$K_2 = \frac{16\sqrt{3}}{9}\Big(\frac{2}{\pi}\Big)^{\frac{1}{6}}\cos(\frac{\pi}{3}) \approx 1.428. \tag{81}$$

The coefficient ω/ω_{pe} varies as the power 2/5 instead of 2/3 for the Vlasov equation and v_{th}/c varies as the power 3/5 instead of 1/3 for the Vlasov equation.

5.2.2 Cold electron case

We now explore the limit $\omega >> kv_{th}$, where the conductivity equation (72) gives

$$\sigma_{yy} = \frac{i\omega_{pe}^2\varepsilon_0}{\sqrt{2\pi}v_{th}^3k^3}\Big[\frac{(3\chi+1)\sqrt{2\pi}k^3v_{th}^3}{2\omega} - \frac{i\pi\omega^4(1-\chi)}{(3\chi-1)^4v_{th}^2k^2}\exp\Big(-\frac{\omega^2}{2v_{th}^2k^2(3\chi-1)^2}\Big)\Big]. \tag{82}$$

This expression has to be compared with the one obtained with the Vlasov equation

$$\sigma_{yy}^{Vlasov} = \frac{i\omega_{pe}^2\varepsilon_0}{v_{th}k\sqrt{2\pi}}\Big[\frac{\sqrt{2\pi}kv_{th}}{\omega} - i\pi\exp\Big(-\frac{\omega^2}{2v_{th}^2k^2}\Big)\Big]. \tag{83}$$

Here, the real part of the conductivity varies as ω_{pe}^2/ω similarly to the Vlasov equation but the imaginary part varies as $\omega_{pe}^2\omega^4/v_{th}^5k^5$ instead of $\omega_{pe}^2/v_{th}k$ for the Vlasov equation. We also observe for the two populations M_1 model, a presence of the term $(3\chi-1)^2$ in the exponential factor instead of 1.

Inserting equation (82) into the impedance equation (59) results in

$$Z = \frac{6\omega^6\omega_{pe}^2\beta}{c^3v_{th}^5\sqrt{2\pi}}\Big(\frac{\sqrt{2}v_{th}(3\chi-1)}{\omega}\Big)^8 - \frac{i\omega}{\sqrt{\omega_{pe}^2\alpha'-\omega^2}}. \tag{84}$$

Using the definition (60), the absorption coefficient is

$$A^{M_1} = \frac{K_3\Big(\frac{v_{th}}{c}\Big)^3\Big(\frac{\omega_{pe}}{\omega}\Big)^2}{\Big[1+\frac{K_3}{4}\Big(\frac{v_{th}}{c}\Big)^3\Big(\frac{\omega_{pe}}{\omega}\Big)^2\Big]^2+\Big[\frac{\omega_{pe}^2}{\omega_0^2}\alpha'-1\Big]^{-\frac{1}{2}}} \tag{85}$$

where K_3 and α' are given by

$$K_3 = \frac{384(3\chi-1)^4(1-\chi)}{\sqrt{2\pi}} \approx 0.822, \tag{86}$$

$$\alpha' = \frac{(3\chi-1)}{2} \approx 0.156. \tag{87}$$

This expression has to be compared with the one obtained with the Vlasov equation [25]

$$A^{Vlasov} = \frac{K_4\Big(\frac{v_{th}}{c}\Big)^3\Big(\frac{\omega_{pe}}{\omega}\Big)^2}{\Big[1+\frac{K_4}{4}\Big(\frac{v_{th}}{c}\Big)^3\Big(\frac{\omega_{pe}}{\omega}\Big)^2\Big]^2+\Big[\frac{\omega_{pe}^2}{\omega_0^2}-1\Big]^{-\frac{1}{2}}} \tag{88}$$

with

$$K_4 = \frac{16}{\sqrt{2\pi}} \approx 6.383. \tag{89}$$

The two expressions of the absorption coefficient are similar but the major difference originates from the parameter α' in the denominator of (85). The coefficient ω/ω_{pe} varies as the power 2 and v_{th}/c varies as the power 3 exactly like in the Vlasov absorption coefficient. The parameter α' in the denominator of the two populations M_1 model absorption makes a significant difference with the Vlasov equation absorption coefficient. While a pole is reached for $\omega/\omega_{pe}=1$ for the Vlasov equation, the pole is reached when $\omega\alpha'/\omega_{pe}=1$ for the two populations M_1 model.
Even if in both limits the absorption phenomenon is captured qualitatively, the results are not satisfactory. This shows the limits of using the two populations M_1 model for studying the laser plasma absorption. The aim of the next part is to see if these results can be improved using the M_2 model.

5.3 M_2 model

In this part the conductivity and the absorption coefficient are calculated with the M_2 model.

In this case the first order moments in the perturbative development F_{1x}, F_{1y}, F_{2xx}, F_{2xy} and F_{2yy} are calculated using (8)

$$F_{1x} = F_{1y} = 0, \tag{90}$$

$$F_{2xx} = \frac{F_0}{3}, \qquad F_{2xy} = 0, \qquad F_{2yy} = \frac{F_0}{3} \tag{91}$$

where F_0 is given by equation (37). On the contrary to the M_1 model closure (15), the M_2 model closure cannot be given explicitly [1]. Nevertheless, only the component f_{3xyx} of the tensor f_3 is required in this study. Using [1, 15, 10], one can show that the linearisation of f_{3xyx} around the equilibrium state (35) gives

$$f_{3xyx} = 0 + \frac{\delta f_{1y}}{5}. \tag{92}$$

The linearisation of the M_2 model (25) leads to

$$\partial_t \delta f_{1y} + \partial_x(\xi \delta f_{2xy}) + \frac{q}{3m}\partial_\xi(F_0 \delta E_y) - \frac{2q\delta E_y F_0}{3m\xi} = 0. \tag{93}$$

Performing a Fourier transform of the previous equation one finds

$$\delta f_{1y} = -i\frac{q\delta E_y}{3m}\frac{\dfrac{\partial F_0}{\partial \xi} - 2\dfrac{F_0}{\xi}}{\omega - \dfrac{\xi^2 k^2}{5\omega}}. \tag{94}$$

Following the method introduced in the two populations M_1 model section, one obtains the conductivity

$$\sigma_{yy} = \frac{i\omega_{pe}^2 \varepsilon_0 \omega}{3v_{th}^5}\sqrt{\frac{2}{\pi}}\left[P\int_0^\infty \frac{\xi^4 \exp(-\frac{\xi^2}{2v_{th}^2})}{\omega^2 - k^2\xi^2\lambda_1}d\xi - \frac{i\pi\omega^3}{2k^5\sqrt[3]{\lambda_1}}\exp\left(\frac{-\omega^2}{2k^2\lambda_1 v_{th}^2}\right)\right] \tag{95}$$

where $\lambda_1 = 1/5$.

The integral in this expression cannot be calculated analytically. In order to perform the complete calculation, two limiting cases are considered: $\omega/k << v_{th}$ and $\omega/k >> v_{th}$.

5.3.1 Hot electron case

Following the method introduced for the two populations M_1 model, the conductivity is

$$\sigma_{yy} = \frac{i\omega_{pe}^2 \varepsilon_0 \omega}{3v_{th}^5\sqrt{\pi}}\Big[-\frac{v_{th}^3}{k^2} - \frac{i\pi\omega^3}{\lambda\sqrt{2\lambda}k^5}\Big] \tag{96}$$

This expression has to be compared with the one obtained with the Vlasov equation σ_{yy}^{Vlasov} (74). Ignoring the constant values, the real part of the conductivity varies in $\omega_{pe}^2\omega/v_{th}^2k^2$ exactly

like for the Vlasov equation and the imaginary part varies in $\omega_{pe}^2\omega^4/v_{th}^5k^5$ instead of $\omega_{pe}^2/v_{th}k$ for the Vlasov equation.

The expression for the M_2 model absorption coefficient reads

$$A = \frac{K_5\Big(\frac{\omega}{\omega_{pe}}\Big)^{\frac{2}{7}}\Big(\frac{v_{th}}{c}\Big)^{\frac{5}{7}}}{\Big[1+\frac{K_5}{4}\Big(\frac{\omega}{\omega_{pe}}\Big)^{\frac{2}{7}}\Big(\frac{v_{th}}{c}\Big)^{\frac{5}{7}}\Big]^2+\Big[\frac{K_5}{4}\Big(\frac{\omega}{\omega_{pe}}\Big)^{\frac{2}{7}}\Big(\frac{v_{th}}{c}\Big)^{\frac{5}{7}}\Big]^2} \tag{97}$$

with

$$K_5 = \frac{49.651\lambda^2\sqrt{\lambda}\cos(\frac{3\pi}{7})}{\pi\sqrt{2\pi}} \approx 0.025. \tag{98}$$

The coefficient ω/ω_{pe} varies as the power 2/7 instead of 2/3 for the Vlasov equation and v_{th}/c varies as the power 5/7 instead of 1/3 for the Vlasov equation.

5.3.2 Cold electron case

In the limit $\omega >> kv_{th}$, the conductivity (95) reads

$$\sigma_{yy} = \frac{i\omega_{pe}^2\varepsilon_0}{v_{th}^5}\Big[\frac{v_{th}^5}{\omega} - \frac{i\omega^4\sqrt{\pi}}{k^5 3\lambda^2\sqrt{2\lambda}}\exp(-\frac{\omega^2}{2k^2\lambda v_{th}^2})\Big] \tag{99}$$

This expression has to be compared with the one obtained with the Vlasov equation (83). In this case the real part of the conductivity varies in ω_{pe}^2/ω like for the Vlasov equation. This good behavior was already obtained with the two populations M_1 model. The imaginary part varies as $\omega_{pe}^2\omega^4/v_{th}^5k^5$ like for the two populations M_1 model, instead of $\omega_{pe}^2/v_{th}k$ for the Vlasov equation but the exponential factor is obtained using the M_2 model contrarily to the two populations M_1 model.

The expression for the M_2 model absorption coefficient reads

$$A = \frac{K_6\Big(\frac{v_{th}}{c}\Big)^3\Big(\frac{\omega_{pe}}{\omega}\Big)^2}{\Big[1+\frac{K_6}{4}\Big(\frac{v_{th}}{c}\Big)^3\Big(\frac{\omega_{pe}}{\omega}\Big)^2\Big]^2+\Big[\frac{\omega_{pe}^2}{\omega^2}-1\Big]^{-\frac{1}{2}}} \tag{100}$$

with

$$K_6 = \frac{128}{5\sqrt{10\pi}} \approx 4.567. \tag{101}$$

This expression is compared with the one obtained from the Vlasov equation (88). The coefficient ω/ω_{pe} varies as the power 2 and v_{th}/c varies as the power 3 exactly like the Vlasov equation absorption coefficient. In opposite to the two populations M_1 model, the pole is reached at $\omega/\omega_{pe} = 1$ like for the Vlasov equation. In this limit, one observes the advantage in using the M_2 model compared to the two populations M_1 model.

The calculation of the impedance Z, has been performed using the conductivity expressions established in the hot and cold electron limits $\omega/k << v_{th}$ and $\omega/k >> v_{th}$. However, equation

(59), implies the integration over all k from minus infinity to infinity. We can consider that the calculation of the impedance, using equation (59), holds if the main contribution of the integral comes from a set of wave numbers k where the limiting expressions for the conductivity are valid. In order to check this assumption, the parameters ω/ω_{pe} and v_{th}/c are fixed and the expression in the integral (59) is analyzed as a function of k.
We present here an example with $\omega/\omega_{pe} = 0.1$ and $v_{th}/c = 0.8$ to illustrate how one can validate our approach for these parameters. The same steps can be used for any choice of parameters in order to verify if the calculated absorption is valid. The modulus integrand of the impedance for the Vlasov equation, the M_2 and M_1 two populations models are displayed in Fig.3, using the expressions derived in the limit $\omega/k << v_{th}$. In this case the dimensionless wave number kc/ω_{pe} must be larger than $(\omega/\omega_{pe})/(v_{th}/c) = 0.125$. Indeed, according to Fig.3 the main contribution to the integral comes from a set of wave numbers where the conductivity expressions are valid. Moreover, the position and the shape of integrand in the case of M_2 model agrees well with the Vlasov result.

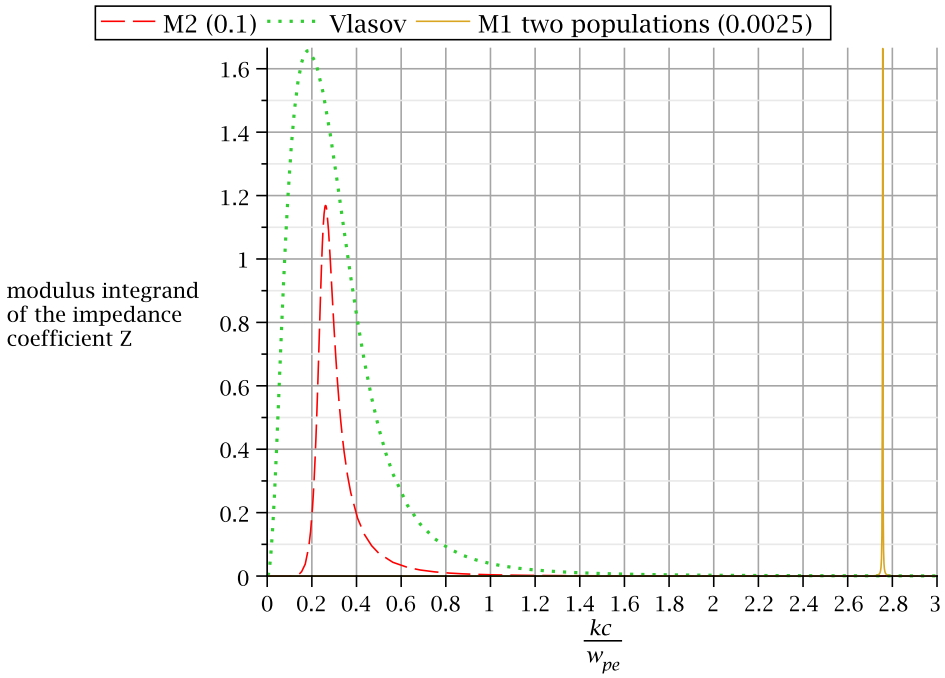

Figure 3: Representation of the modulus integrand of the impendance (59) as a function of k in the limit $\omega/k << v_{th}$ in the case $\omega/\omega_{pe} = 0.1$ and $v_{th}/c = 0.8$. The modulus integrand has been multiplied by a factor 0.1 for the M_2 model and by 0.0025 for the M_1 two populations model.

A second example is displayed in Fig.4, with $\omega/\omega_{pe} = 0.3$ and $v_{th}/c = 0.1$ using the expressions established in the limit $\omega/k >> v_{th}$. In this case, the dimensionless wave number kc/ω_{pe} must be smaller than $(\omega/\omega_{pe})/(v_{th}/c) = 3$. Indeed, one can verify in Fig.4 that the main contribution to the integral comes from a set of wave numbers where the conductivity expressions are valid.

In conclusion, it has been shown that the M_1 model is not able to model the skin effect of an electromagnetic wave in an overdense plasma. In the limit $\omega/k << v_{th}$, the two populations M_1 and the M_2 moments models both capture the absorption phenomenon qualitatively, but do not describe it correctly. In the opposite limit $\omega/k >> v_{th}$, the absorption phenomenon is not captured correctly by the two populations M_1 model. The M_2 model, on the contrary, correctly

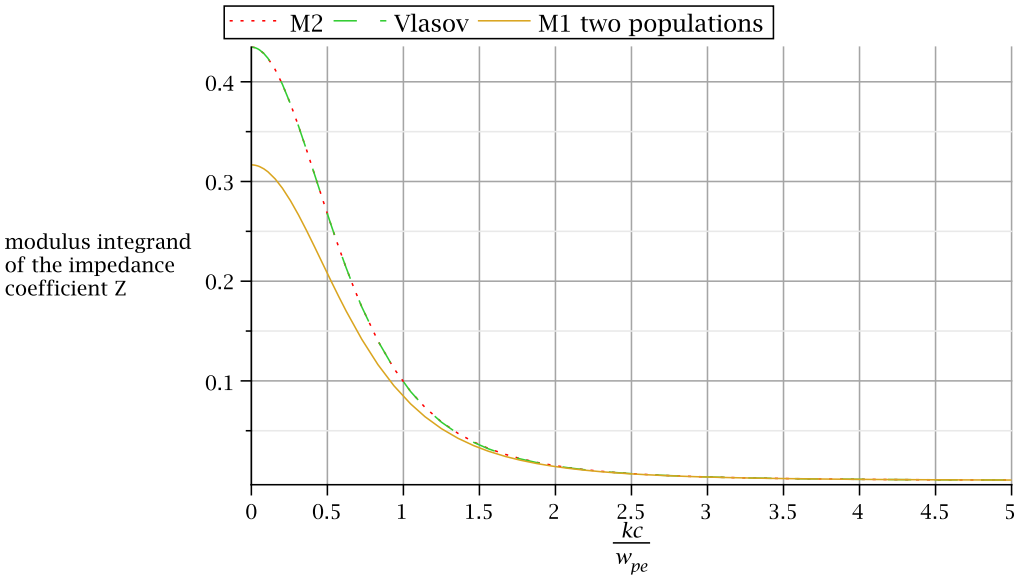

Figure 4: Representation of the modulus integrand of the impendance coefficient as a function of wave number in the limit $\omega/k >> v_{th}$ in the case $\omega/\omega_{pe} = 0.3$ and $v_{th}/c = 0.1$.

captures the phenomenon and the absorption expression obtained is very close to the one followed from the Vlasov equation. This study shows the limits of the three models for studies of the laser plasma absorption. Higher moments models must therefore be used to correctly describe this phenomenon. In the hot electron lmit, the M_3 model could be tested but the calculation is beyond the scope of this study.

6 Conclusion

The particle beams interaction, Landau damping and collisionless skin effect have been studied using the M_1, the two populations M_1 and M_2 moments models. By analytically deriving the dispersion relations, we have demonstrated that the particle beams interaction is correctly captured by the moments models. The Landau damping is also captured by the three models, but the M_1 model is inaccurate while the two populations M_1 and M_2 moments models describe it accurately. The electromagnetic wave absorption coefficients in the case of collisionless skin effect have been calculated with the three models. We have shown that the M_1 model is not able to model the absorption phenomenon. Two limit cases have been considered. In the case $\omega/k << v_{th}$, the two populations M_1 and the M_2 moments models both capture the absorption phenomena results but they are inaccurate. In the second case, $\omega/k >> v_{th}$, the two populations M_1 model does not describe correctly the absorption effect while the M_2 model is sufficiently accurate. Higher moments models such as the M_3 moments or full kinetic models can be used to correctly describe the absorption phenomenon in both limits. This work demonstrates through the Landau damping and the laser-plasma absorption that angular moments models have to be used carefully. These models do not always behave as a full kinetic model and can suffer from a severe lack of accuracy depending on the phenomenon studied. This study can be extended to other plasma effects and also to take into account collisional processes.

Acknowledgments. The authors are grateful to M. Touati for interesting discussions on the topic.

References

[1] G.W. Alldredge, C.D. Hauck, and A.L. Tits. High-order entropy-based closures for linear transport in slab geometry II: A computational study of the optimization problem. SIAM Journal on Scientific Computing Vol. 34-4 (2012), pp. B361-B391.

[2] C. Berthon, P. Charrier, and B. Dubroca. An HLLC Scheme to Solve The M1 Model of Radiative Transfer in Two Space Dimensions. J. Sci. Comput. 31 347-89 (2007).

[3] A.V Brantov, V.Yu Bychenkov, O.V.Batishchev, and W.Rozmus. Nonlocal heat wave propagation due to skin layer plasma heating by short laser pulses. Computer Physics communications 164 67, 2004.

[4] O. Buneman. Phys. Rev.115, 503 (1959).

[5] F. Chen. *Introduction to Plasma Physics and Controlled Fusion.* Plenum Press, New York, 1984.

[6] J.F. Drake, P.K. Kaw, Y.C. Lee, G. Schmidt, C.S. Liu, and M.N. Rosenbluth. Parametric instabilities of electromagnetic waves in plasmas. Phys. Fluids 17, 778, 1974.

[7] B. Dubroca, J.-L. Feugeas, and M. Frank. Angular moment model for the Fokker-Planck equation. European Phys. Journal D, 60, p 301, 2010.

[8] B. Dubroca and J.L. Feugeas. étude théorique et numérique d'une hiéarchie de modèles aux moments pour le transfert radiatif. C. R. Acad. Sci. Paris, t. 329, SCrie I, p. 915-920, 1999.

[9] B. Dubroca and J.L. Feugeas. Entropic moment closure hierarchy for the radiative transfert equation. C. R. Acad. Sci. Paris Ser. I, 329 915, 1999.

[10] C.P.T. Groth and J.G. McDonald. Towards physically-realizable and hyperbolic moment closures for kinetic theory. Continuum Mech. Thermodyn. 21, 467-493 (2009).

[11] C. Hauck and R. McLarren. Positive P_N closures. Siam J. Sci. Comp. 32, 2603.

[12] C.D. Hauck. High-order entropy-based closures for linear transport in slab geometry. Commun. Math. Sci 9 (1), 187-205 (2011).

[13] N. Krall and A. Trivelpiece. Principles of Plasma Physics, McGraw Hill, New York 1973.

[14] L. D. Landau. J. Phys. USSR 10, 26 (1946).

[15] C.D. Levermore. Moment closure hierarchies for kinetic theories. J. Stat. Phys. 83, 1021-1065 (1996).

[16] E. M. Lifshitz and L. P. Pitaevskii. Plasma Kinetics, Pergamon Press, 1981.

[17] D. Lynden-Bell. Statistical mechanics of violent relaxation in stellar systems. Mon. Not. R. Astr. Soc., 136 (1967), 101–121.

[18] J. Mallet, S. Brull, and B. Dubroca. An entropic scheme for an angular moment model for the classical Fokker-Planck-Landeau equation of electrons. Comm. Comput. Phys. 422, 2013.

[19] J. Mallet, S. Brull, and B. Dubroca. General moment system for plasma physics based on minimum entropy principle. In revision.

[20] J. H. Malmberg and C. B. Wharton. Phys. Rev. Lett. 13, 184 (1964).

[21] A. Marocchino, M. Tzoufras, S. Atzeni, A. Schiavi, Ph. D. Nicolaï, J. Mallet, V. Tikhonchuk, and J.-L. Feugeas. Nonlocal heat wave propagation due to skin layer plasma heating by short laser pulses. Phys. Plasmas 20, 022702, 2013.

[22] J.G. McDonald and C.P.T. Groth. Towards realizable hyperbolic moment closures for viscous heat-conducting gas flows based on a maximum-entropy distribution. Continuum Mech. Thermodyn. 25, 573-603 (2012).

[23] G.N. Minerbo. Maximum entropy Eddigton Factors. J. Quant. Spectrosc. Radiat. Transfer, 20, 541, 1978.

[24] I. Muller and T. Ruggeri. Rational Extended Thermodynamics. Springer, New York (1998).

[25] W. Rozmus, V. T. Tikhonchuk, and R. Cauble. A model of ultrashort laser pulse absorption in solid targets. Phys. Plasmas 3, 360 (1996).

[26] H. Struchtrup. Macroscopic Transport Equations for Rarefied Gas Flows. Springer, Berlin (2005).

[27] M. Touati, J.L. Feugeas, P. Nicolaï, J.J. Santos, L. Gremillet, and V.T. Tikhonchuk. New Journal of Physics 16 (2014).

[28] R. Turpault, M. Frank, B. Dubroca, and A. Klar. Multigroup half space moment appproximations to the radiative heat transfer equations. J. Comput. Phys. 198 363 (2004).